International Journal of Emerging Technology in Computer Science & Electronics (IJETCSE)
ISSN: 0976-1353 Volume 24 Issue 5 – APRIL 2017.

A BRIDGELESS BUCK BOOST BIDIRECTIONAL PFC CONVERTER FOR PLUG IN VEHICLES

Bharathi.R[#1] ,Kamalnath.K[#2],Karthikeyan.G[#3],Meena.G[#4] and S.Shanmugapriya[*5]

[#1]*UG Student, Electrical and Electronics Engineering, Parisutham Institute of Technology and Science,Thanjavur, India*

[#2]*UG Student, Electrical and Electronics Engineering, Parisutham Institute of Technology and Science,Thanjavur, India*

[#3]*UG Student, Electrical and Electronics Engineering, Parisutham Institute of Technology and Science,Thanjavur, India*

[#4]*UG Student, Electrical and Electronics Engineering, Parisutham Institute of Technology and Science,Thanjavur, India*

[*5] *Assistant Professor, Electrical and Electronics Engineering, Parisutham Institute of Technology and Science,Thanjavur, India*

Abstract— ***This paper proposes a bidirectional bridgeless totem-pole interleaved power-factor-correction (PFC) converter using SiC MOSFETs as the front-end stage of an onboard charger for plug-in electric vehicles (PEVs). The proposed converter provides bidirectional operation enabling both grid-to-vehicle (G2V) charging and vehicle-to-grid (V2G) ancillary services. The converter is suitable for efficient G2V V2G onboard charging due to its superiorities in terms of bidirectional operation, smaller current ripple, lower EMI, lower conduction losses and switching losses. A 3.3kW PFC converter is designed and developed, using Silicon-Carbide MOSFETs with fast recovery body diodes, for validation of and V2G operating modes. Utilizing SiC MOSFETs enables continuous current mode (CCM) operation of the totem-pole PFC converter in high-power applications. The converter is capable of converting 85Vac-265Vac line voltages into a regulated dc voltage in the range of 300V to 600V. The maximum efficiency of converter reaches up to 99.2% with 0.99 power factor.***

***Index Terms*—About four key words or phrases in alphabetical order, separated by commas.**

I. INTRODUCTION

In a typical plug-in electric vehicle (PEV), a single-phase power factor correction (PFC) ac-dc converter is used as the front-end stage of an onboard grid-to-vehicle (G2V) charger, followed by an isolated dc-dc converter as the second stage, as illustrated in Fig. 1 [1]-[3]. The most commonly used PFC converter in an onboard charger is a single-phase diode bridge rectifier followed by a boost converter. It converts the 85Vac~265Vac single-phase ac voltages to a regulated dc voltage (typically around 390V) [4]-[6].

Although the conventional PFC boost converter is the most popular topology, its efficiency suffers from the conduction losses of the front-end diode bridge rectifier and it is not bidirectional [7]. Therefore, bridgeless PFC boost converters are investigated to reduce the number of diodes and increase the efficiency [8]-[16]. Moreover, bridgeless topologies can be slightly modified to enable bidirectional operation to provide vehicle-to-grid (V2G) ancillary services. Dual boost bridgeless PFC converter is a commonly used bridgeless topology, but its serious common mode noise requires a large electromagnetic interference (EMI) filter [8]-[10]. Semi-boost bridgeless PFC converter can reduce the common mode noise; however, each of its two bridges has to handle the peak input current, increasing the size and cost of the components [11], [12]. A dual boost bridgeless PFC converter using bidirectional switches is also considered by researchers [13]; however, its major drawbacks include difficult gate drive design and the inefficient post-end diode rectifier.

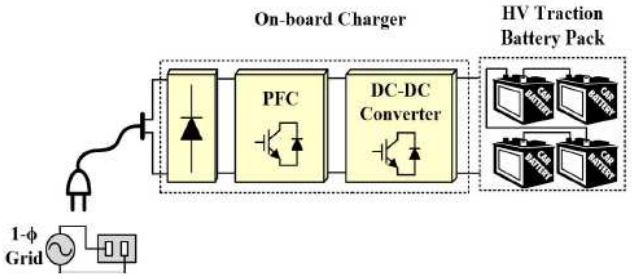

Fig.1.Typical onboard charger with a front end PFC stage in a PEV Power factor

Another variant topology of dual boost bridgeless PFC is the pseudo totem-pole bridgeless PFC converter [14]. However, the difficult control and gate drive design limit its practical implementation. Totem-pole bridgeless PFC converter, shown in Fig. 2(a), overcomes the issues of other bridgeless topologies [15], [16]. However, reverse recovery issue of Silicon (Si) MOSFET's intrinsic body diodes causes large reverse recovery current in continuous current mode (CCM) and makes it impractical for high power applications. Fast recovery diodes can be used in anti-parallel, but they increase the size and cost of the converter.

This paper introduces a Silicon-Carbide (SiC) based bridgeless totem-pole interleaved PFC converter as the front-end stage of an onboard charger capable of G2V and V2G operating modes. In comparison to other topologies, the proposed topology has superiorities in terms of high efficiency, small common mode noise, small ac current ripple, small reverse recovery current, less number of components, simple control and simple gate drive design. The low reverse recovery charge of SiC body diode and the low turn-on resistance of SiC MOSFET make the converter an efficient and cost effective solution for bidirectional onboard chargers. The converter is capable of interfacing with 85Vac-265Vac universal single-phase ac-line voltages.

Furthermore, due to the high voltage capability of SiC MOSFETs, depending on the input voltage, the dc link voltage can be regulated in the range from 300V to 600V.

II. LITERATURE SURVEY

The situation in the automotive industry is such that the demands for higher fuel economy and more electric power are driving advanced vehicular power system voltages to higher levels[1].Research and development efforts have focused on developing advanced powertrains and efficient energy system[2]. The impending global energy crisis has opened up new opportunities for the automotive industry to meet the ever-increasing demand for cleaner and fuel-efficient vehicles[3].This is the result of increasingly sophisticated engine and body controls, as well as the introduction of new ,electrically controlled functions[4].The fuel efficiency and performance of novel vehicles with electric propulsion capability are largely limited by the performance of the energy storage system(ESS)[5].

III. BRIDGELESS INTERLEAVED PFC CONVERTER

The proposed bidirectional bridgeless totem-pole interleaved CCM PFC converter using six SiC MOSFETs is shown in Fig. 2(b). Two boost interleaved phases (*L1*, *S1*, *S2* and *L2*, *S3*, *S4*) are driven with 180 degrees phase difference. In each boost phase, the high-side switch and the low-side switch are driven complementarily with a dead band.

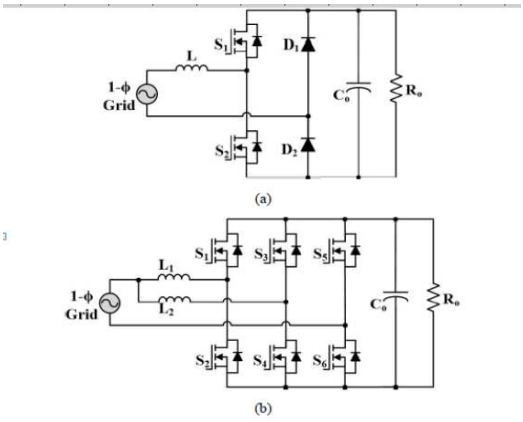

Fig.2.a)Unidirectional bridgeless buck-boost DCM PFC converter .Fig.2.b) Proposed bidirectional bridgeless buck-boost interleaved CCM PFC converter

Two line rectification diodes are replaced with two SiC MOSFETs (*S5* and *S6*) to be used for synchronous rectification.

The operation principles of one leg of totem-pole interleaved PFC converter for G2V charging is depicted in Fig. 3. In the positive half-cycle of ac line, as shown in Fig. 2(a), *S6* is turned on, connecting the low potential of ac line to the dc ground. When *S2* is turned on, the ac source charges the inductor *L1*. The current of *L1* increases linearly,

$$\frac{di_{L1}}{dt} = \frac{v_{ac}}{L_1}$$

When *S2* is turned off, a deadband interval is introduced before *S1* is turned on to avoid overshoot current. After the dead band, *S1* is turned on, as shown in Fig.2(b), generating a freewheeling path for inductor current and discharging the stored energy in inductor to the dc link. The current of *L1* decreases linearly according to Eq. (2),

$$\frac{di_{L1}}{dt} = \frac{v_{ac} - V_o}{L_1}$$

The turn-on time of *S2* is determined by the boost duty ratio of pulse-width-modulation (PWM) signal, while the turn-on time of *S1* is complementary to *S2*.

In the negative half-cycle of ac line, *S5* is turned on, connecting the high potential of ac line to the dc link. When *S1* is turned on, as shown in Fig. 3(c), the ac source charges the inductor *L1*, and the current increases linearly as Eq. (1). *S2* is turned on after *S1* is turned off with a deadband interval, which enables synchronous rectification and generates a freewheeling path for inductor current, as shown in Fig. 3(d). The inductor current decreases linearly as Eq. (2). In the negative half-cycle of ac line, the turn-on time of *S1* is determined by the boost duty ratio.

S3 and *S4* are used to construct the second interleaved phase, driven with 180 degrees phase difference with respect to *S1* and *S2*. The operation of the second interleaved phases is similar to that of the first interleaved phase, increasing the effective switching frequency by two times.

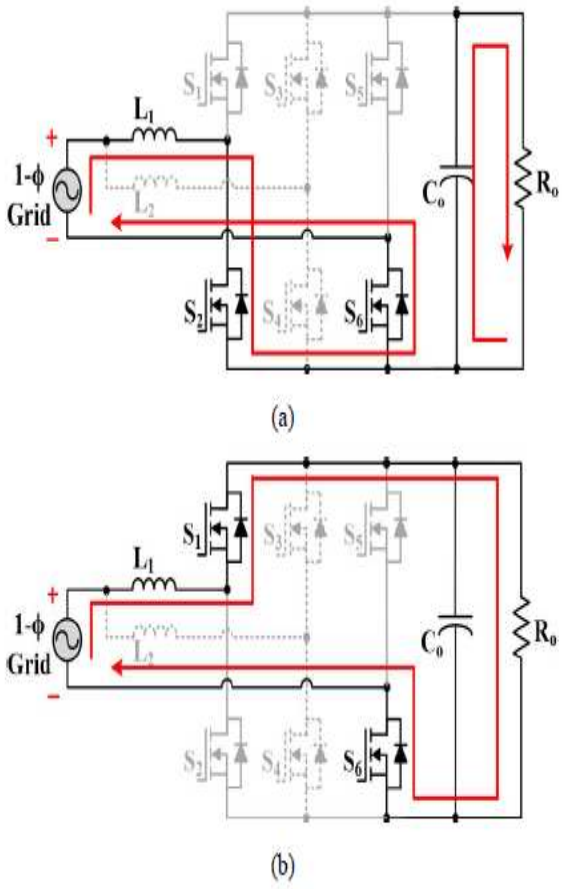

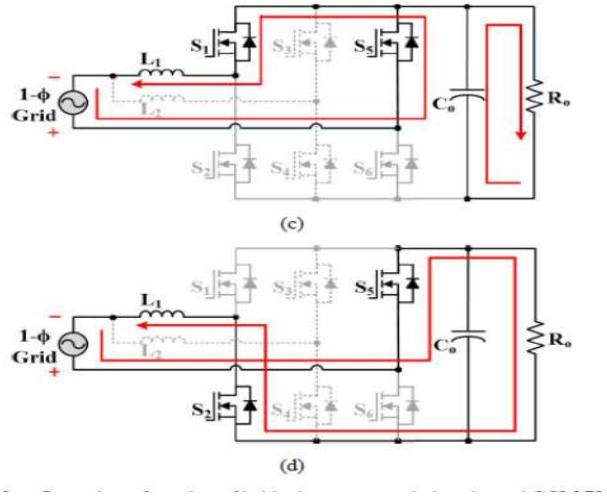

Fig.3.Opeeration of one leg of bridgeless buck-boost interleaved CCM PFC converter for G2V operation

For V2G operation, the switching operation modes are similar to those of G2V. In the positive half-cycle of ac line, as shown in Fig. 3.*S6* is turned on, connecting the low potential of ac line to the dc ground. When *S1* is turned on, the dc link charges the inductor *L1*. The current of *L1* increases linearly according to Eq. (3),

$$\frac{di_{L1}}{dt} = \frac{V_o - v_{ac}}{L_1}$$

When *S1* is turned off, *S2* is turned on with a dead band interval in between, as shown in Fig. 3(b). The inductor current freewheels through *S2* and releases the stored energy to the ac line. The current of *L1* decreases linearly,

$$\frac{di_{L1}}{dt} = -\frac{v_{ac}}{L_1}$$

The turn-on time of *S1* is determined by the buck duty ratio of pulse-width-modulation (PWM) signal, while the turn-on time of *S2* is complementary to *S1*. In the negative half-cycle

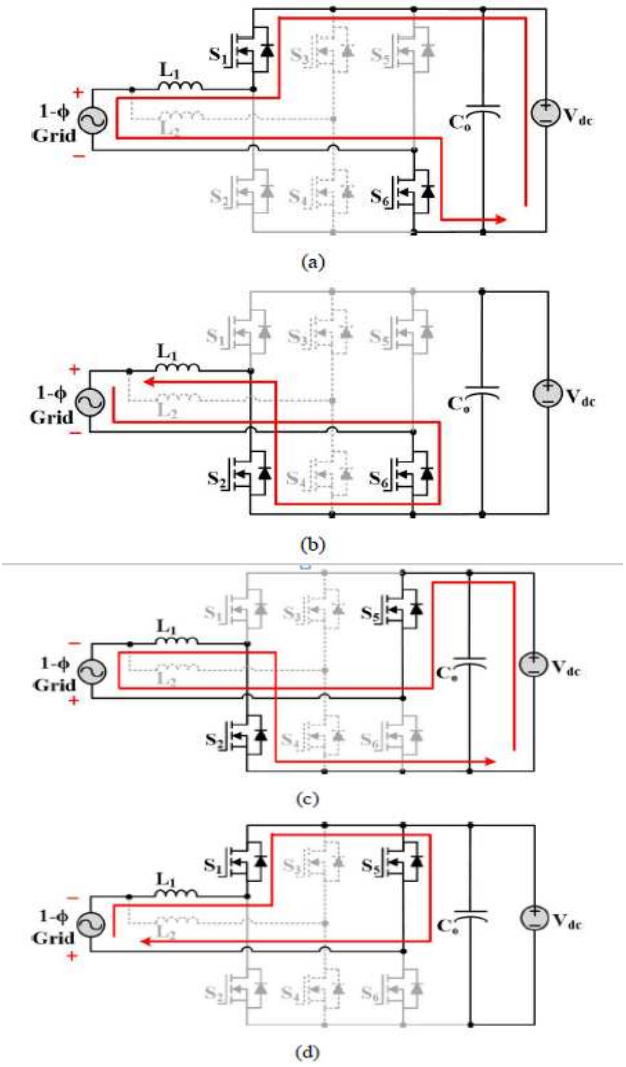

Fig.4.Operation of one leg of bridgeless buck-boost interleaved CCM PFC converter for V2G operation

Of ac line, *S5* is turned on, connecting the high potential of ac line to the dc link. The dc link charges the inductor *L1* when *S2* is turned on, as shown in Fig. 3(c). *S1* is turned on after *S2* is turned off to enable synchronous rectification, as shown in

Fig. 3(d). In the negative half-cycle of ac line, the buck PWM duty ratio determines the turn-on time of *S2*.

By introducing a current reference, 180 degree out of phase with respect to the ac line voltage, the turn-on time of switches can be determined by the buck PWM duty ratio. Therefore, the inductor current can be shaped 180 degree out of phase with respect to the ac line voltage.

IV. DESIGN AND GUIDELINE AND CONTROL SCHEME

A. DC Link Voltage Range

For universal input line voltages (85Vac-265Vac), the dc link voltage can be varied in the range of 300V to 600V. The minimum dc link voltage is regulated at 380V when the ac-line voltage is 155Vac-265Vac. When the ac-line voltage is 85Vac-155Vac, the maximum dc link voltage is regulated at 525V. Therefore, a high-voltage traction battery (200V-

420V) can be charged using a second stage dc-dc resonant converter with 0.5-0.8 voltage gain [17]. The dc link voltage variation can alleviate the need for a wide voltage gain range for the second stage, which in turn reduces the design difficulty and increases the efficiency of the second stage of an onboard charger.

B. PFC Interleaved Inductors

The interleaved inductors are designed to meet the requirement of high power factor over a wide range of ac-line voltages. Two non-coupled inductors are used. The inductance value of inductors should be high enough to avoid discontinuous current mode (DCM) operation of each boost leg and acquire high power factor, low total harmonic distortion (THD) and low electromagnetic interference (EMI). As the inductance value of an inductor decreases at higher operating currents, the nominal value of inductance is designed at maximum operating current, corresponding to full load condition (3.3kW) at lower line voltage (85Vac).

The inductance value is determined by the switching frequency, which is set at 100kHz, and the current ripple of each boost leg, which is selected to be equal to 20% (Δi) of the maximum ac current, yielding

$$L_1 = L_2 = \frac{V_{ac,\min}^2}{\Delta_i P_{o,\max} f_{sw}}\left(1 - \frac{\sqrt{2}V_{ac,\min}}{P_{o,\max}}\right)$$

The maximum current through the inductor can be calculated as

$$I_{L1,\max} = I_{L2,\max} = \frac{\sqrt{2}P_{o,\max}}{2V_{ac,\min}}\left(1 + \frac{\Delta_i}{2}\right)$$

In this work, 70μ permeability Kool Mutoroid cores from Magnetics Inc. are used, which are wound up with 32 turns of 1.5mm litz wire. The inductance value is 340μH under no load and 100μH under full load at low line-voltage. The dc resistance is around 30mΩ.

C. DC-link Capacitor

The capacitance value of dc-link capacitor is determined by the low frequency voltage ripple and the loading hold-up time. The capacitor needs to be large enough to suppress the voltage ripple (as small as 10% (Δv) of minimum dc link voltage) caused by low-frequency line voltage.

In addition, the capacitor is required to store enough energy to hold up the dc-link voltage above its minimum value for 20ms (thold) under full load, yielding

$$C_o = \frac{2P_{o,\max}t_{hold}}{V_{o,\max}^2 - V_{o,\min}^2}$$

Therefore, the capacitance of dc link capacitor is set at 880μF. In this work, two 220μF/400V aluminum capacitors are connected in series to handle 600V. Eight groups of such series-connected capacitors are connected in parallel to create 880μF.

D. SiC MOSFETs

MOSFET selection is considered based on (1) high drain-to-source breakdown voltage; (2) low turn-on

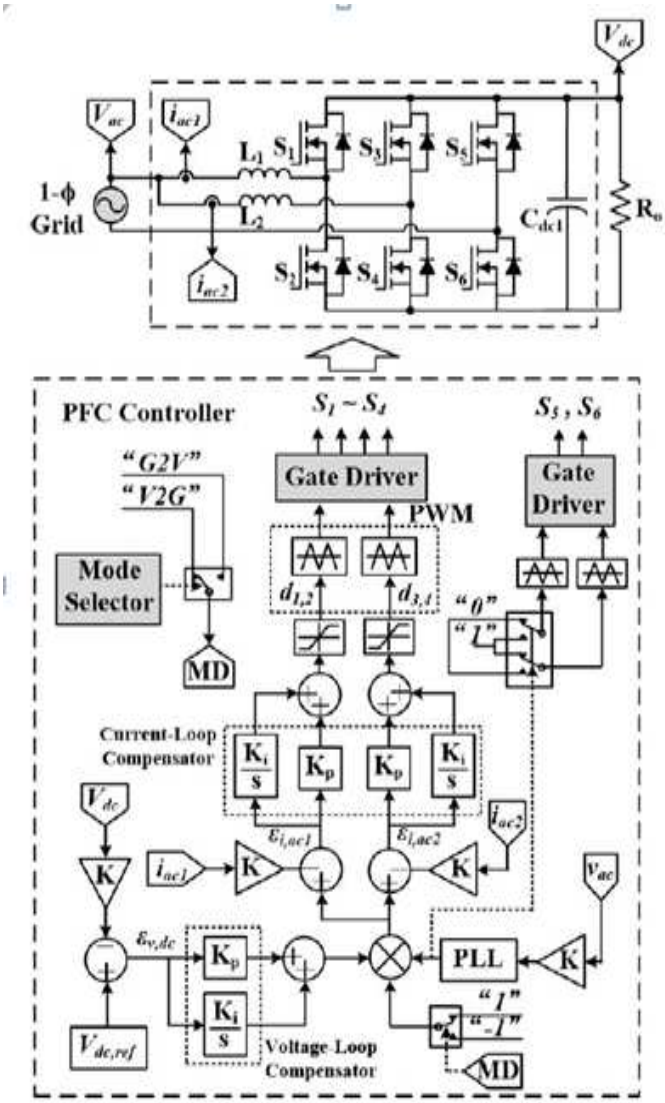

Fig.5.PFC control loop for the bridgeless totem-pole interleaved PFC coverter

A resistance; (3) fast switching turn-on and turn-off times; (4) low gate charge; (5) small parasitic output capacitance; and (6) fast reverse recovery body diode. SiC power MOSFETs (C2M0160120D) from CREE are selected due to their superiorities in terms of high voltage capability, low turn-on resistance and low reverse recovery charge of body diode. In this work, six SiC FETs (1200V/36A) are used. They are able to handle voltage spikes twice of maximum dc-link voltage. 80mΩ turn-on resistance reduces the conduction losses. The reverse recovery charge of body diodes is 192nC, in comparison to typical 2μC for a counterpart Si body diode, making it suitable for PFC high power CCM operation.

$$C_o = \frac{P_{o,\max}}{\Delta_v 2\pi f_{ac} V_{o,\min}^2} \quad (7)$$

$$(8)$$

E. Control Scheme

A dual closed-loop pulse-width-modulation (PWM) control, as shown in Fig. 5, is used to control the ac-dc interleaved PFC stage. During G2V operation, the ac-line voltage *vac* is sampled, and a phase-locked-loop (PLL) is used to create a reasonably accurate sinusoidal ac-line current reference. The dc-link voltage (*Vdc*) is sampled and controlled through a voltage-loop compensator to regulate the magnitude of ac-line current reference. By adjusting the

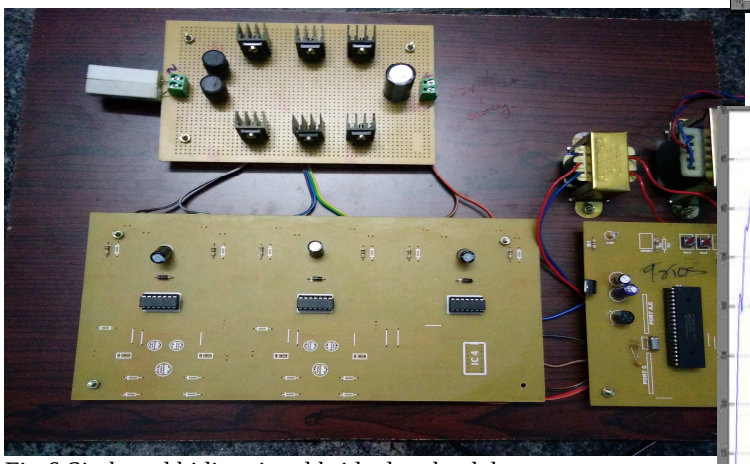

Fig.6.Sic-based bidirectional bridgeless buck boost interleaved PFC converter

Ac-line current magnitude or input power, the dc-link voltage can be regulated at *Vdc ,ref*. Inductor current of each interleaved phase (*iac1* or *iac2*) is individually sampled and controlled through a current loop compensator to shape a sinusoidal inductor current. Inductor current, rather than ac-line current, is regulated to ensure equal current sharing in two interleaved phases and achieve fast response.

Two compensated duty cycles (*d1,2*: *d1=1-d2*; *d3,4*: *d3=1-d4*) are generated by each current-loop compensator. Due to the operation of proposed topology, the duty cycles have abrupt changes between "0" to "1" at ac line zero-crossing. By comparing the duty cycles to triangle carrier signals, four PWM signals are then generated to control *S1~S4*. To achieve synchronous rectification, *S5* and *S6* are turned on or turned off complimentarily based on the polarity of ac-line voltage.

V.During V2G operation, a negative feedback is introduced to the ac-line current reference to shape a sinusoidal ac current with 180o phase difference with respect to the ac-line voltage.

VI. EXPERIMENTAL RESULT

A 3.3kW prototype of the proposed SiC-based bridgeless PFC stage, as illustrated in Fig. 6, is designed and developed to validate the operation of the converter. The converter is capable of converting 86Vac-265Vac universal single-phase ac-line voltages into a regulated dc-link voltage in the rane of

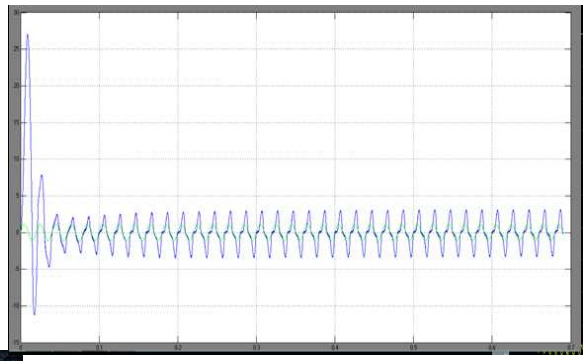

Fig.7.Waveform of Input voltage

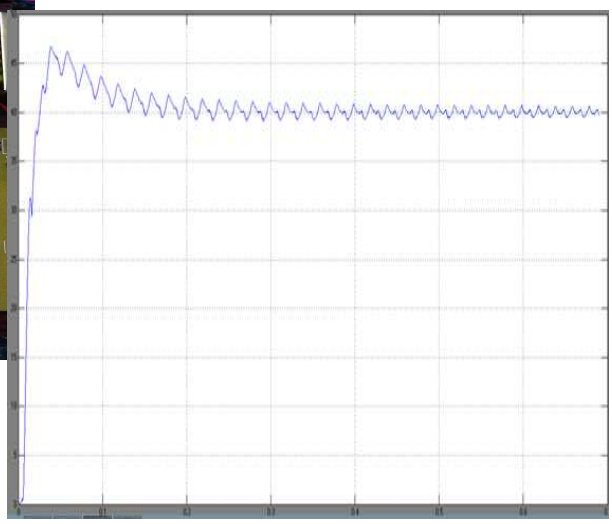

Fig.8. Waveform of Output voltage and current

300V to 600V. With consideration of efficiency and power density, the switching frequency is selected at 100kHz. The circuit specifications are listed in Table I.

The proposed ac-dc PFC stage is tested for performance evaluation of converting both high-voltage and low-voltage ac-line voltages. Fig. 7(a) illustrates the ac-line voltage, ac current and boost-phase inductor current of the PFC stage at 110Vac/60Hz ac-line voltage during G2V charging at 1.5kW. In order to avoid current spikes, a soft start is generated at every ac-line zero-crossing by setting a number of disabled switching cycles. The dc-link voltage is regulated at 420V with a 20V/120Hz ripple, which is 5% of the dc-link voltage. The PFC stage is then connected with a second stage dc-dc converter. The voltage and current waveforms of the PFC stage at 220Vac/60Hz ac-line voltage, 2kW G2V charging are shown in Fig. 7(b). The dc-link voltage ripple is reduced to 15V, which is 3.5% of dc-link voltage. At 2kW, the G2V efficiency can reach up to 98.8% at 220Vac/60Hz ac-line voltage. The power factor is close to 0.99.

A load step change is set from 1.2kW to 700W to evaluate the dynamic response of the converter. The ac-line current drops from 10A to 6.4A. The dc current of the PFC stage drops from 4A to 2.6A. It takes 0.18 seconds, corresponding to 10 ac-line cycles, to regulate the dc-link voltage. Fig. 8 shows the charger dynamic response of load step change (from 1.2kW to 700W). Fig. 9 demonstrates the efficiency of

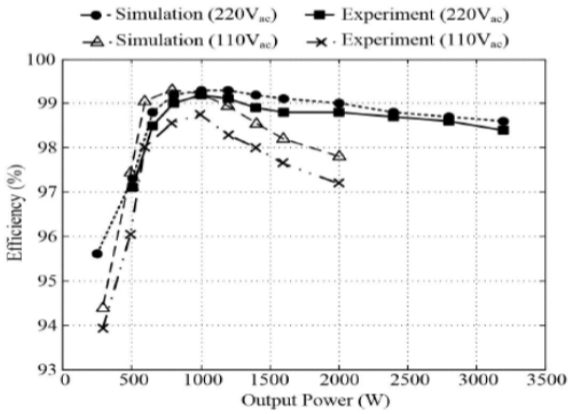

Fig.9.Simulation and experimental efficiencies of the proposed PFC converter at different ac-line voltages and output power

proposed converter for 110Vac and 220Vac input voltages. As shown in this figure, the simulation results adequately coincide with the experimental measurements.

VII. CONCLUSION

This paper outlines a SiC-based bidirectional bridgeless totem-pole interleaved PFC converter as the front-end stage of an onboard charger for PEVs. Due to its bidirectional operation, the proposed converter is suitable for both G2V charging and providing V2G ancillary services. SiC MOSFETs with fast recovery body diodes significantly reduce the reverse recovery current, making the topology a cost effective solution for CCM operation in high power applications. A 3.3kW PFC converter is designed and developed for validation of onboard charging. Experimental results are carried out to validate its capability of converting 85Vac-265Vac line voltages into a regulated dc voltage in the range from 300V to 600V. The measured efficiency reaches up to 98% at 110Vac line voltage and 1.5kW charging; and 98.8% at 220Vac line voltage and 2kW charging.

.

REFERENCES

[1] A. Emadi, S. S. Williamson, and A. Khaligh, “Power electronics intensive solutions for advanced electric, hybrid electric, and fuel cell vehicular power systems,” IEEE Trans. Power Electron., vol. 21, no. 3, pp. 567-577, May 2006.

[2] C. C. Chan, A. Bouscayrol, and K. Chen, “Electric, hybrid, and fuel-cell vehicles: Architectures and modeling,” IEEE Trans. Veh. Technol., vol. 59, no. 2, pp. 589-598, Feb. 2010.

[3] A. Khaligh and S. Dusmez, “Comprehensive topological analysis of conductive and inductive charging solutions for plug-in electric vehicles,” IEEE Trans. on Veh. Technol., vol. 61, no. 8, pp. 3475-3489, Oct. 2012.

[4] J. G. Kassakian, “Future automotive electrical systems-The power electronics market of the future,” in Proc. IEEE Appl. Power Electron. Conf., New Orleans, LA, 2000, pp. 3-9.

[5] S.M. Lukic, J. Cao, R.C. Bansal, F. Rodriguez, and A. Emadi, “Energy Storage Systems for Automotive Applications,” IEEE Trans. on Ind. Electron., vol. 55, no. 6, pp. 2258-2267, 2008.

[6] H. Wang, S. Dusmez, and A. Khaligh, “Design and analysis of a full bridge LLC based PEV charger optimized for wide battery voltage range,” IEEE Trans. on Veh. Technol., vol. 63, no. 4, pp. 1603-1613, May 2014.

[7] J. P. M. Figuerido, F. L. Tofili, and B. L. A. Silva, “A review of single-phase PFC topologies based on the boost converter,” in Proc. IEEE Int. Conf. Indus. Appl., Sao Paulo, Brazil, Nov. 2010, pp. 1-6.

[8] H. Ye, Z. Yang, J. Dai, C. Yan, X. Xin, and J. Ying, “Common mode noise modeling and analysis of dual boost PFC circuit,” in Proc. Int. Telecommun. Energy Conf. (INTELEC), Sep. 2004, pp. 575-582.

[9] B. Lu, R. Brown, and M. Soldano, “Bridgeless PFC implementation using one cycle control technique,” in Proc. IEEE App. Power Electron. (APEC) Conf., Mar. 2005, pp. 812-817.

[10] P. Kong, S. Wang, and F.C. Lee, “Common mode EMI noise suppression in bridgeless boost PFC converter,” in Proc. CPES Power Electron. Conf., Apr. 2006, pp. 65-70.

[11] F. Musavi, W. Eberle, and W. G. Dunford, “A high-performance single-phase bridgeless interleaved PFC converter for plug-in hybrid electric vehicle battery chargers,” IEEE Trans. on Ind. Appl., vol. 47, no. 4, pp. 1183-1143, 2011.

[12] F. Musavi, W. Eberle, and W. G. Dunford, “A phase shifted semi-bridgeless boost power factor corrected converter for plug-in hybrid electric vehicle battery chargers,” in Proc. IEEE Appl. Power Electron. Conf. and Expo., 2011, pp. 821 828.

[13] D. Tollik and A. Pietkiewicz, “Comparative analysis of 1-phase active power factor correction topologies,” in Proc. Int. Telecommun. Energy Conf. (INTELEC), Oct. 1992, pp. 517-523.

[14] L. Huber, Y. Jang, and M. M. Jovanovic, “Performance evaluation of bridgeless PFC boost rectifiers,” IEEE Trans. on Power Electron., vol. 23, no. 3, pp. 1381-1390, May 2008.

[15] S. S. Darly, P. V. Ranjan, K. V. Bindu, and B. J. Rabi, “A novel dual boost rectifier for power factor improvement,” Int. Conf. on Elec. Energy Syst., 2011, pp. 121-127.

[16] B. Su, J. M. Zhang, and Z.Y. Lu, “Totem-pole boost bridgeless PFC rectifier with simple zero-current detection and full-range ZVS operating at the boundary of DCM/CCM,” IEEE Trans. on Power Electron., vol. 26, no. 2, pp. 427-435, Feb. 2011.